Please cite this article in press as: Merz et al., Autoproteolytic and Catalytic Mechanisms for the β-Aminopeptidase BapA—A Member of the Ntn Hydrolase Family, Structure (2012), http://dx.doi.org/10.1016/j.str.2012.07.017

Structure
Article

Autoproteolytic and Catalytic Mechanisms for the β-Aminopeptidase BapA—A Member of the Ntn Hydrolase Family

Tobias Merz,[1,4] Tobias Heck,[2,5] Birgit Geueke,[2] Peer R.E. Mittl,[1] Christophe Briand,[1] Dieter Seebach,[3] Hans-Peter E. Kohler,[2] and Markus G. Grütter[1,*]
[1]Biochemistry Institute, University of Zürich, Winterthurerstrasse 190, 8057 Zürich, Switzerland
[2]Department of Environmental Microbiology, Swiss Federal Institute of Aquatic Science and Technology (Eawag), Überlandstrasse 133, 8600 Dübendorf, Switzerland
[3]Laboratory of Organic Chemistry, Department of Chemistry and Applied Biosciences, Hönggerberg HCI, Wolfgang-Pauli-Strasse 10, 8093 Zürich, Switzerland
[4]Present address: NovAliX, BioParc, bld Sébastien Brant BP 30170, F-67405 Illkirch Cedex, France
[5]Present address: Swiss Federal Laboratories for Materials Science and Technology (Empa), Lerchenfeldstrasse 5, 9014 St. Gallen, Switzerland
*Correspondence: gruetter@bioc.uzh.ch
http://dx.doi.org/10.1016/j.str.2012.07.017

SUMMARY

The β-aminopeptidase BapA from *Sphingosinicella xenopeptidilytica* belongs to the N-terminal nucleophile (Ntn) hydrolases of the DmpA-like family and has the unprecedented property of cleaving N-terminal β-amino acid residues from peptides. We determined the crystal structures of the native $(\alpha\beta)_4$ heterooctamer and of the 153 kDa precursor homotetramer at a resolution of 1.45 and 1.8 Å, respectively. These structures together with mutational analyses strongly support mechanisms for autoproteolysis and catalysis that involve residues Ser250, Ser288, and Glu290. The autoproteolytic mechanism is different from the one so far described for Ntn hydrolases. The structures together with functional data also provide insight into the discriminating features of the active site cleft that determine substrate specificity.

INTRODUCTION

The class of β-aminopeptidases so far comprises five functionally characterized hydrolytic enzymes, i.e., three BapA variants from *Sphingosinicella xenopeptidilytica* 3-2W4 (Geueke et al., 2005), *S. microcystinivorans* Y2 (Geueke et al., 2006), and *Pseudomonas sp.* MCI3434 (Komeda and Asano, 2005) as well as BapF from *Pseudomonas aeruginosa* PAO1 (Fuchs et al., 2011), and DmpA from *Ochrobactrum anthropi* (Fanuel et al., 1999b). These enzymes share the exceptional ability to cleave synthetic β-peptides, which consist of backbone-elongated β-amino acid residues that are not processed by common proteolytic enzymes (Frackenpohl et al., 2001; Geueke and Kohler, 2007; Wiegand et al., 2002). Due to their structural properties and high resistance against proteolysis, β-peptides are considered promising building blocks for the design of novel peptidomimetics (Aguilar et al., 2007; Seebach and Gardiner, 2008). To our knowledge, the first and so far only structure of an enzyme with β-aminopeptidase activity is DmpA (Bompard-Gilles et al., 2000). DmpA has an αββα-sandwich architecture, which is strongly reminiscent of the fold of classical Ntn hydrolases (Brannigan et al., 1995). Nevertheless, DmpA is classified as a novel member of the Ntn hydrolase family due to a different connectivity of the secondary structure elements (Bompard-Gilles et al., 2000; Oinonen and Rouvinen, 2000).

Ntn hydrolases, in general, are synthesized as inactive precursor polypeptides with or without a periplasmic leader sequence. They undergo posttranslational autoproteolytic cleavage into heterodimers. The primary nucleophile that initiates this cleavage is either a serine, threonine or cysteine residue, which, upon self-processing, becomes the essential N-terminal nucleophile for the catalytic activity. This autoproteolytic activation step is a characteristic trait of all Ntn hydrolases (Brannigan et al., 1995; Kim et al., 2003; Saarela et al., 2004; Michalska et al., 2008). Ntn hydrolases occur in different oligomeric states, such as heterodimers (e.g., penicillin G acylase; McVey et al., 2001), heterotetramers (e.g., glutamyltranspeptidase from *Helicobacter pylori*; Boanca et al., 2006), heterooctamers (e.g., penicillin V acylase from *Bacillus sphaericus*; Suresh et al., 1999) or, exceptionally, as very large assembly in the proteasome (Baumeister and Lupas, 1997). Most Ntn hydrolases catalyze the hydrolysis of amide bonds. However, their substrate specificities vary considerably. The ornithine acetyltransferase from the clavulanic-acid-biosynthesis gene cluster (*orf6*) is an exception. This enzyme has the same fold as DmpA, but catalyzes the reversible transfer of an acetyl group from N-acetylornithine to glutamate (Elkins et al., 2005). Among the Ntn hydrolases, penicillin and cephalosporin acylases as well as β-aminopeptidases have particularly high potential for biocatalytic conversions (Bruggink et al., 1998; Barends et al., 2004; Heck et al., 2007, 2009, 2010).

The enzymatic activities of β-aminopeptidases strongly depend on the nature of the N-terminal amino acid of the substrate peptide. While DmpA hydrolyzes D- and L-configured α-amino acid amides, esters and peptides as well as peptides carrying small N-terminal β-amino acids such as β-homoglycine

Please cite this article in press as: Merz et al., Autoproteolytic and Catalytic Mechanisms for the β-Aminopeptidase BapA—A Member of the Ntn Hydrolase Family, Structure (2012), http://dx.doi.org/10.1016/j.str.2012.07.017

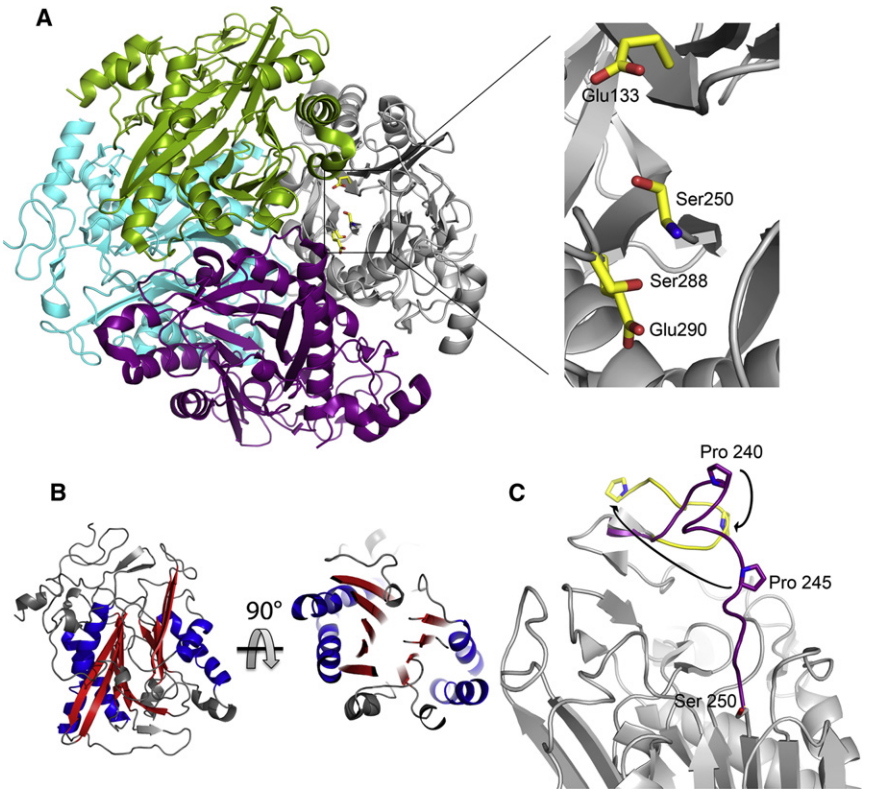

Figure 1. Structural Overview of Native BapA and proBapA

(A) Cartoon representation of the $(\alpha\beta)_4$-BapA heterooctamer. The individual subunits, each comprising an α- and a β-polypeptide chain, are shown in gray, magenta, cyan, and green. The blow-up frame shows the catalytically important residues Glu133, Ser250, Ser288, and Glu290 of the gray subunit as sticks.

(B) Cartoon representation of one αβ subunit. The secondary structure elements contributing to the Ntn fold are colored in red and blue.

(C) Active-site pocket of BapA before and after the autoproteolytic cleavage: Native BapA and pro-BapA are shown in gray. Residues 237–245 of native BapA are depicted in yellow and residues 237 to 249 of proBapA are shown in magenta. The catalytic nucleophile Ser250 is highlighted as sticks. Residues Pro240 and Pro245 are located within a helical loop conformation in proBapA, which upon autoproteolytic processing assume a β sheet-like conformation in the native enzyme. The positional changes of these two residues are indicated by arrows.

and β^3-homoalanine (Fanuel et al., 1999a; Heck et al., 2006), BapA from *S. xenopeptidilytica* exhibits hydrolytic activity with strict preference for variable N-terminal β-amino acids and, remarkably, does not hydrolyze α-peptides (Geueke et al., 2006; Heck et al., 2006). Until now, the natural substrates of β-aminopeptidases remain unknown and structural data about exclusively β-peptide-cleaving enzymes is not available.

Here, we present the high-resolution crystal structures of the β-aminopeptidase BapA, which has exclusive catalytic activity for β-peptide substrates. Our comprehensive structural and functional study about this novel aminopeptidase includes the crystal structures of the active form, its precursor and of the active form in complex with the serine-peptidase inhibitor 4-(2-aminethyl) benzenesulfonyl fluoride (AEBSF, trade name pefabloc SC). The analysis of these BapA structures provides insight into the mechanisms of precursor self-processing and substrate cleavage, and shows the determinants of the enzyme's substrate specificity. Moreover, our mutational analysis indicates that BapA, DmpA, and other so far not characterized DmpA-like aminopeptidases, do not, as reported, act with a "Ser-only" active-site configuration. Instead of a single catalytically active amino acid residue, these enzymes seem to employ a highly conserved Glu-Ser-Ser triad for the self-processing as well as for the catalytic substrate hydrolysis.

RESULTS

Crystal Structure of Native BapA

BapA crystallized in the space group $P2_1$ and contained one $(\alpha\beta)_4$ heterooctameric molecule (153 kDa) in the asymmetric unit. The high-resolution crystal structure (1.45 Å) of BapA was determined by molecular replacement as described in Experimental Procedures. Each heterodimer comprises a large α-polypeptide chain (residues 1–249) and a small β-polypeptide chain (residues 250–373). The molecule adopts a globular disk-like shape with subunits arranged in D_2 symmetry (Figure 1A). Each αβ subunit adopts an αβ βα-sandwich fold that is formed by two layers of four and five mixed β sheets flanked by two helices on each side (Figure 1B). The connectivity of the secondary structure elements in BapA differs from the classical Ntn hydrolase fold, but it is identical to the fold of DmpA. The total interface area between all subunits comprises 7,880 $Å^2$ in BapA and suggests a very stable and permanent octameric state in solution that was elucidated experimentally by gel filtration (data not shown). The model was refined to final R and R_{free} values of 13.5% and 15.3%, respectively. Crystallographic data are listed in Table 1. The BapA molecule contains four active sites, each of which is located at the interface of three adjacent subunits forming the substrate-binding pockets. In analogy to other Ntn hydrolases, Ser250 becomes the N-terminal catalytic nucleophile of the β-polypeptide chain after self-processing (Figure 1C). Glu133, Ser250, Ser288, and Glu290, that we propose to participate in substrate binding and the catalytic mechanism, are located in the same subunit (Figure 1A). A water molecule ($B_{average}$ = 18.1 ± 1.1 $Å^2$) is in close contact to the carboxyl group of Glu133 in each of the active sites. The shape of the active sites of BapA with their buried catalytic residues excludes the action of associated peptidases that could be involved in the precursor cleavage.

Crystal Structure of the Unprocessed BapA Precursor—proBapA

The homotetrameric unprocessed precursor form of BapA (proBapA) was produced with Ser250 mutated to alanine

Table 1. Data Collection and Refinement Statistics—Molecular Replacement

	proBapA	Native BapA	BapA-Pefabloc SC
Data Collection			
Space group	$P2_12_12_1$	$P2_1$	$P2_1$
Cell dimensions			
a, *b*, *c* (Å)	99.7, 113.7, 126.0	87.4, 96.7, 101.4	87.4, 96.8, 101.3
α, β, γ (°)	90, 90, 90	90, 108.2, 90	90,108.4,90
Resolution (Å)[a]	29.4–1.8 (1.9–1.8)	48.8–1.45 (1.47–1.45)	48.0–1.8 (1.9–1.8)
R_{sym} or R_{merge}	7.1 (47.3)	4.2 (43.3)	10.0 (49.7)
$I / \sigma I$	15.6 (4.0)	17.0 (2.7)	12.9 (3.1)
Completeness (%)	99.1 (99.2)	98.5 (92.3)	97.6 (94.7)
Redundancy	4.40 (4.46)	3.24 (2.33)	3.78 (3.70)
Refinement			
Resolution (Å)	1.8	1.45	1.8
No. reflections	131,659	278,534	144,691
R_{work} / R_{free}	15.5/18.0	13.5/15.3	16.0/19.0
No. atoms			
Protein	10,639	21,935 (10,836)[b]	10,708
Ligand/ion	49	83	238
Water	1,124	1,741	1,265
B-factors			
Protein	21.54	18.58 (17.31)[b]	19.61
Ligand/ion	37.59	30.61	27.85
Water	31.79	31.06	29.48
Rmsds			
Bond lengths (Å)	0.009	0.011	0.007
Bond angles (°)	1.138	1.445	1.05
PDB Accession Code	3N5I	3N2W	3N33

[a]Values in parentheses correspond to the highest-resolution outer shell.
[b]Without hydrogen atoms. One crystal was used for each data set.

(S250A mutant), which prevents the primary cleavage of the enzyme subunits into α- and β-polypeptides. This enzymatically inactive form of BapA crystallized in the space group $P2_12_12_1$ and contains one homotetrameric molecule in the asymmetric unit. The high-resolution crystal structure (1.8 Å) of proBapA was determined by molecular replacement as described in Experimental Procedures. The model was refined to final R and R_{free} values of 15.5% and 18.0%, respectively. Crystallographic data are listed in Table 1. Overall, the globular shape and the contact area between the subunits in proBapA strongly resemble native BapA. The location of the linker peptide connecting the designated α and β chains (residues 231–249) represents the major structural difference between native BapA and proBapA (Figure 1C). In proBapA, this segment partly covers the active site region in native BapA. The linker polypeptide is flexible in three subunits and in one subunit adopts a helical conformation due to crystal contacts with Pro240 and Pro245. In native BapA, the same segment is moved out of the active site cleft and adopts a β sheet-like conformation with the prolines located in turns. Cleavage of the Asn249-Ser250 peptide bond goes along with a subtle reorientation of the Ser250 side chain, which represents a second functionally highly important structural change in the active site. Comparing the conformations of Ala250 in proBapA and Ser250 in active BapA we find that Ser250 is rotated around its C-Cα bond upon self-processing. This rotation reduces the distance between Ala/Ser250 and Ser288-Oγ from 3.67 to 2.79 Å in native BapA (Figures 2A and 2B). The interresidue distances between Glu133, Glu290, and Ser288 do not significantly differ between the precursor and the processed enzyme.

Catalytic Residues for Self-Processing and Catalysis

We exchanged six amino acid residues in the vicinity of the catalytic nucleophile Ser250 for Ala residues, creating the BapA point mutants E133A, K248A, N249A, S250A, S288A, and E290A. The consequences of these mutations on the autoproteolysis of the precursor polypeptide were judged based on the time-dependent appearance of individual α and β chains on SDS-PAGE gels. Native BapA was already fully processed after purification, while the BapA mutants did not self-process at all or only partially within 192 hr (Table 2; Figure 3). In fact, the exchange of Ser250, Ser288, or Glu290 for alanine completely abrogated precursor cleavage: neither could the individual α- and β-polypeptide chains be detected on SDS-PAGE gels (Figure 3) nor did the mutant enzymes exhibit any residual enzymatic activity after 192 hr of incubation (Table 2). The BapA mutants E133A, K248A, and N249A were clearly delayed in self-processing (SDS-PAGE gel for K248A not shown). Nevertheless, activity measurements after 192 hr of incubation revealed that K248A and N249A mutants were as active as native BapA, whereas the exchange of Glu133 completely abolished enzymatic activity (Table 2).

Because the BapA mutants E133A, S250A, S288A, and E290A did not undergo the complete processing step, the effects of these mutations on substrate binding and conversion could not be investigated. In order to study the mechanism of substrate cleavage independently from precursor processing, we coexpressed the individual α- and β-polypeptide chains of BapA from a Duet expression vector and introduced the same mutations that were previously investigated for their effects on self-processing. We ensured by sequence analysis that the newly introduced N-terminal methionine residue of the β-polypeptide chain was posttranslationally removed by *Escherichia coli* (data not shown). The cell-free extracts containing the respective BapA Duet mutants were then tested for their catalytic activity with the chromogenic substrate H-β^{3}hAla-*p*NA. The mutants E133A Duet and S250A Duet are inactive, whereas the mutants S288A Duet and E290A Duet exhibit <1% and 24% residual activity, respectively, compared to wild-type BapA Duet (Table 2).

Mechanism of Self-Processing

In the commonly accepted self-processing mechanism for Ntn-hydrolases the catalytic nucleophile attacks the carbonyl carbon atom of the preceding peptide bond. This results in the formation of a tetrahedral intermediate that is decomposed with an ester bond being formed and the carbonyl carbon amide nitrogen bond cleaved. In a second step, the ester bond is hydrolyzed, resulting in an α- and a β-polypeptide chain with the free N-terminal

Please cite this article in press as: Merz et al., Autoproteolytic and Catalytic Mechanisms for the β-Aminopeptidase BapA—A Member of the Ntn Hydrolase Family, Structure (2012), http://dx.doi.org/10.1016/j.str.2012.07.017

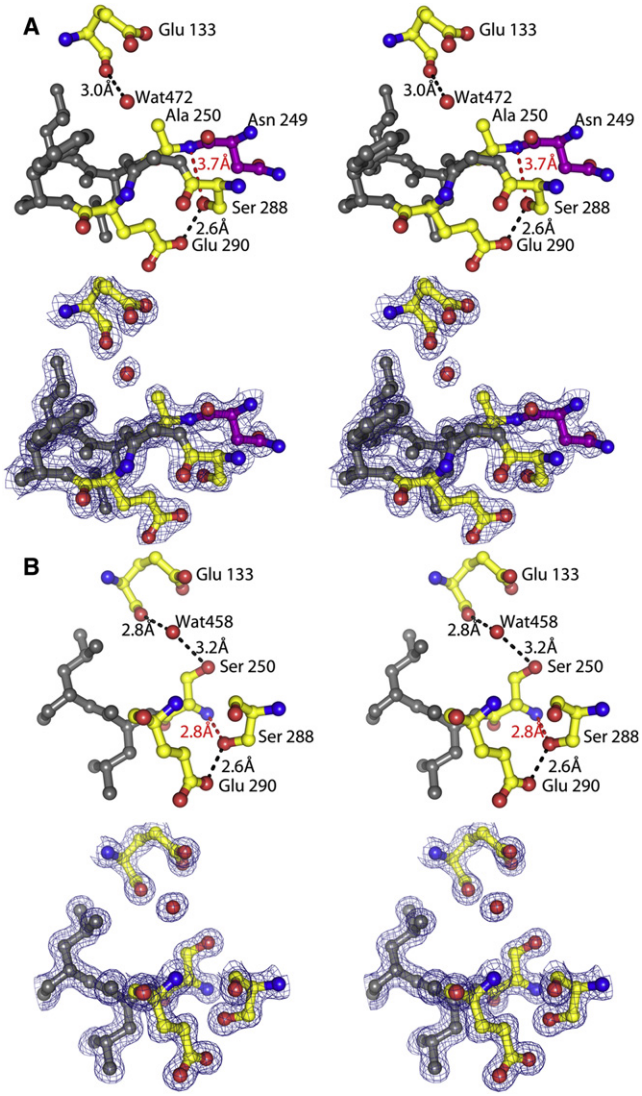

Figure 2. Stereoview of the Active Sites of proBapA and Native BapA

(A) BapA precursor mutant S250A (proBapA): The important catalytic residues Glu133, Ser288, Glu290, and Ala250 are shown as sticks and the catalytic water molecule is shown as a red sphere. The carboxy-terminal residue of the α chain before the autoproteolytic cleavage is shown in magenta. In the bottom panel the same part of the structure is shown with the 2fo-fc electron density map contoured at 1.5 σ.

(B) Native BapA: rotation of Ser250 around the C-Cα-bond decreases the $NH_3^+{}_{250}$-OH_{288} distance from 3.7 to 2.8 Å (distance values highlighted in red in figures A and B). In the bottom panel the same part of the structure is shown with the 2fo-fc electron density map contoured at 1.5 σ.

catalytic nucleophile. This mechanism requires a conformational strain on the peptide bond (Johansson et al., 2009) and, in addition, includes a flip of the peptide preceding the bond to be cleaved. It was deduced from structural information of the proform and active form of glycosylasparaginase (Xu et al., 1999) and cephalosporin acylase (Kim et al., 2006). This so called N-O shift mechanism is unlikely to occur in BapA for the following structural reasons: (1) Ser250-Oγ when modeled in the Ala250 mutant structure would require to adopt an eclipsed conformation, which is not in an ideal geometry to attack the preceding main chain carbonyl carbon of Asn249, (2) the Asn249-Ser250 scissile peptide bond in proBapA is completely planar and unstrained, (3) the cleavage-defective BapA mutants S288A and E290A indicate a critical involvement of these residues in the processing mechanism besides Ser250, (4) a peptide flip of the scissile peptide bond between Asp249 and Ser250 results in an energetically unfavorable conformation. All these features are characteristic for BapA and DmpA-type Ntn-hydrolases and distinguish them from other Ntn-hydrolases for which the N-O acyl shift mechanism was proposed. Based on the structural data and our mutational studies, we propose the following self-processing mechanism (Figure 4): Ser288-Oγ is the nucleophile that is in an ideal position to attack the carbonyl carbon of the Asn249-Ser250 scissile peptide bond (Figure 4A). The peptide carbonyl group of Asn249 draws a proton from the side-chain OH of Ser250 leaving a partial negative charge on the Ser250-Oγ. The nucleophilic attack of Ser288 is facilitated by the transfer of a proton from Ser288-Oγ to the neighboring carboxyl side chain of Glu290. The tetrahedral intermediate formed (Figure 4B) is stabilized by a hydrogen bond to Ser250-Oγ. This intermediate collapses with the cleavage of the original Asn249-Ser250 peptide bond resulting in the formation of the new N-terminal Ser250 α-amino group of the β-polypeptide and the N-terminal α-polypeptide, which is ester-linked to the side chain of Ser288. In a second step the water oxygen—ideally positioned through H-bonds with Asn207-Nδ and the amide nitrogen of Leu135—is the nucleophile that attacks the ester carbonyl carbon atom. This leads to the hydrolysis of the ester bond and to the release of the α-polypeptide. Ser288-Oγ subsequently binds the proton back from Glu290. This proposed mechanism is clearly different from the *cis*-autoproteolysis described recently by (Buller et al., 2012): modeling of a *cis*-conformation could not be accommodated in the presented structure, moving residues far away from their canonical conformation.

Catalytic Mechanism of Substrate Cleavage

The substrate molecule freely diffuses into the active-site pocket of BapA and its N terminus makes electrostatic interactions with the side chain carboxyl group of Glu133 (Figure 5B, Michaelis complex). Such an interaction is observed in the structure of BapA in complex with the inhibitor Pefabloc (Figure 5A). When positioning a β-peptide substrate in the active site accordingly the following substrate-cleavage mechanism can be deduced: Glu290 activates Ser250-Oγ via Ser288-Oγ and the α-amino group of Ser250 for the nucleophilic attack on the carbonyl carbon atom of the substrate's scissile peptide bond. Leu135-NH and Asn207-NH_2 form the oxyanion hole and stabilize the negative charge of the oxyanion of the tetrahedral intermediate (Figure 5B), which collapses to the acyl enzyme under release of the C-terminal substrate moiety. The hydrolysis of the acyl enzyme is subsequently catalyzed by the water molecule, which is hydrogen bonded to the N-terminal α-amino group of Ser250. The structure of the inhibitor Pefabloc bound in the active site of BapA (Figure 5A) allows to model how substrate binds in the active site and supports the here described mechanism (Heck et al., 2012).

Please cite this article in press as: Merz et al., Autoproteolytic and Catalytic Mechanisms for the β-Aminopeptidase BapA—A Member of the Ntn Hydrolase Family, Structure (2012), http://dx.doi.org/10.1016/j.str.2012.07.017

Table 2. Mutations in BapA and Their Impact on Precursor Cleavage and Substrate Hydrolysis

Residue	Point Mutation	Precursor Cleavage (Autoproteolysis)	Enzymatic Activity (Catalysis)	Residue Essential for	
				Autoproteolysis	Catalysis
	wt	Complete	100%[a]		
Glu133	E133A	Slow	Inactive[a,b]	No	Yes
Lys248	K248A	Slow	100%[a]	No	No
Asn249	N249A	Slow	100%[a]	No	No
Ser250	S250A	No cleavage	Inactive[b]	Yes	Yes
Ser288	S288A	No cleavage	<1%[b]	Yes	Yes
Glu290	E290A	No cleavage	24%[b]	Yes	Yes

[a]The activities of the mutants with partially purified enzymes were measured after 192 hr of incubation under standard assay conditions (see Experimental Procedures). 100% correspond to the activity of partially purified native BapA that was treated under the same conditions.
[b]The activities of the BapA Duet variants were measured under standard assay conditions from cell-free extracts containing the recombinantly expressed enzymes. 100% correspond to the activity of cell-free extract containing native BapA Duet (see Experimental Procedures).

Comparison between the Substrate-Binding Pockets of BapA and DmpA

The superposition of the structures of native BapA, DmpA (PDB ID 1B65), and a so far uncharacterized protein from *Pyrococcus horikoshii* (PH0078, PDB ID 2DRH) show a good overlap of the corresponding catalytic residues. However, the sizes of the substrate-binding pockets differ notably (Figure 5C). In BapA, a 3_{10}-helix comprising the residues Glu120 to Arg126 creates a wide substrate-binding pocket, which is largely occluded by loops in DmpA (Gln131 to Trp137) and PH0078 (Glu120 to Ser128). From this superposition we conclude that Trp137, which points into the active-site cavity of DmpA, restricts catalysis of DmpA to the removal of sterically undemanding N-terminal amino acids from peptides. To confirm this hypothesis, we exchanged Trp137 of DmpA for alanine by site-directed mutagenesis in order to widen the substrate-binding pocket of DmpA and thus make it accessible for bulkier substrates. Hereby, it is important to mention that the point mutation W137A negatively affected the self-processing rate of the DmpA precursor polypeptide into the individual α- and β-polypeptides. In contrast to the native BapA and DmpA proteins that were fully processed after the purification procedure, DmpA W137A was only half-processed after purification and 3 days of incubation at pH 7.2 and 37°C. A survey of the kinetic parameters of the conversion of the β^3-homoamino acid *p*-nitroanilides H-βhGly-*p*NA, H-β^3hAla-*p*NA, H-D-β^3hAla-*p*NA, H-β^3hPhe-*p*NA, and H-D-β^3hPhe-*p*NA by BapA, DmpA, and DmpA W137A is shown in Table 3. While BapA converted the aromatic β^3-homophenylalanine *p*-nitroanilides of L- and D-configuration with k_{cat}/K_M values of 14,500 and 940 $M^{-1}s^{-1}$, respectively, the conversion of these bulky substrates by DmpA was negligible (k_{cat}/K_M < 10 $M^{-1}s^{-1}$). The single amino acid exchange of Trp137 for alanine in DmpA drastically altered the substrate specificity of DmpA W137A leading to more than 280- and 670-fold increased catalytic efficiencies for the conversion of the substrates H-β^3hPhe-*p*NA and H-D-β^3hPhe-*p*NA, respectively. On the other hand, DmpA W137A converted substrates with small side chains, i.e., H-βhGly-*p*NA, H-β^3hAla-*p*NA, and H-D-β^3hAla-*p*NA, less efficiently than wild-type DmpA and displayed overall k_{cat}/K_M values similar to BapA for these substrates (Table 3).

Sequence Comparison of Putative β-Aminopeptidases and Implications on Their Substrate Specificity

In addition to the five functionally characterized β-aminopeptidases (Geueke et al., 2006; Komeda and Asano, 2005; Fuchs et al., 2011; Fanuel et al., 1999a; Heck et al., 2006), a BLAST search revealed a large number of protein sequences showing high similarity to the sequence of BapA from *S. xenopeptidilytica*. They mainly originated from Gram-negative bacteria, among them many pathogenic species such as *Burkholderia mallei*, *B. pseudomallei* and various strains of *Pseudomonas aeruginosa*, but also from archaea (e.g., *Pyrococcus horikoshii*), fungi (e.g., *Aspergillus oryzae*), and yeast (e.g., *Yarrowia lipolytica*). Strikingly, the region downstream of the N-terminal catalytic nucleophile (ranging from Ser250 to Ser290) and the region around the salt bridge-forming residue Glu133 are highly conserved among all compared sequences, indicating that these regions are crucial for catalysis (Figure 6). Glutamate at position 290 of BapA is less, but functionally conserved. In contrast to these highly conserved regions, the compared sequences show great variability over a stretch of 15–20 amino acids upstream of Glu133. This sequence stretch corresponds to the active-site loop (3_{10}-helix in BapA), which defines the width of the enzymes' substrate-binding pockets and their substrate specificities (Table 3).

DISCUSSION

Reconsideration of the Single-Residue Catalytic Mechanism of DmpA-like Proteins

In this study, we report the crystal structures of the native and precursor form of BapA, a β-aminopeptidase from *S. xenopeptidilytica*. Native BapA revealed a heterooctameric organization comprising four heterodimers in a globular D_2-symmetry arrangement. Each heterodimer assumed an αββα-sandwich fold, which was very similar to the core-fold of classical Ntn hydrolases (Brannigan et al., 1995; Oinonen and Rouvinen, 2000). ProBapA revealed a homotetrameric organization with the same globular arrangement and core-fold as the native enzyme. The displacement of the linker segment between the α- and β-polypeptides (residues 231–249) represented the major structural difference between native BapA and proBapA.

Please cite this article in press as: Merz et al., Autoproteolytic and Catalytic Mechanisms for the β-Aminopeptidase BapA—A Member of the Ntn Hydrolase Family, Structure (2012), http://dx.doi.org/10.1016/j.str.2012.07.017

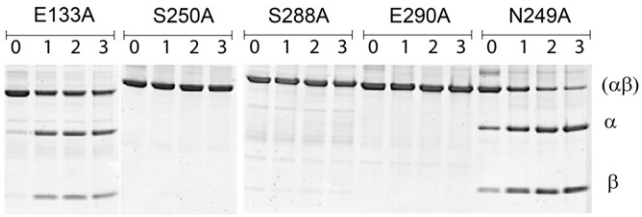

Figure 3. SDS-PAGE Analysis of Five Processing-Deficient or Slow-Processing BapA Point Mutants

The partially purified mutant proteins (0.6 mg/ml) were incubated in 50 mM Tris/HCl buffer (pH 8) at 37°C. Samples were taken after 0 hr (0), 54 hr (1), 120 hr (2), and 192 hr (3). The mutants S250A, S288A, and E290A did not self-process at all, while the mutants E133A and N249A partially processed over 192 hr.

Although this segment contained two prolines in allowed *Ramachandran* regions and no further significant deviations from ideal geometry, we expect these prolines to provide the initial driving force for the large conformational change from a helical to a β sheet-like conformation in the autoprocessing step. Similar observations of strained conformations of linker sequences with prolines that are supposed to regulate the autoprocessing of Ntn hydrolases are reported for glutaryl 7-aminocephalosporanic acid acylase (Kim et al., 2003) and cephalosporin acylase (Kim et al., 2006).

BapA differs from other classical Ntn hydrolases by the connectivity of the secondary structural elements, but has the same fold as DmpA from *O. anthropi* (Bompard-Gilles et al., 2000). Therefore, BapA belongs to the DmpA-like family. DmpA is reported to be structurally closely related to the superfamily of Ntn hydrolases and to exhibit a single-residue catalytic mechanism, in which the N-terminal nucleophile (Ser250), located at the N terminus of the central β sheet, uses its own α-amino group as Brønsted base for activation (Bompard-Gilles et al., 2000).

BapA and DmpA share 41.8% sequence identity and are structurally and biochemically closely related. The catalytically important residues of BapA overlap extremely well with corresponding conserved amino acids of DmpA and the substrate profiles of both enzymes are similar (Heck et al., 2006). We therefore propose that substrate conversions by DmpA and BapA involve a similar mechanism. We showed that the residues Ser250, Ser288, and Glu290 of BapA (corresponding to Ser250, Ser288, and Asp290 of DmpA) have important functions for the self-processing and the catalytic mechanism (Table 2). The crystal structure of native BapA revealed short hydrogen-bond distances of 2.8 Å between Ser250-NH_3^+ and Ser288-OH and of 2.6 Å between Ser288-OH and the carboxyl group of Glu290, suggesting that Glu290 and Ser288 activate the catalytic nucleophile Ser250-Oγ via the α-amino group. These assumptions are in accordance with our kinetic analysis that showed 100- and 4-fold decreased activities, when Ser288 and Glu290 were exchanged for alanines, respectively. Nevertheless, the residual catalytic activity of the S288A Duet mutant indicates that Ser250 alone is capable of being catalytically active as postulated by Bompard-Gilles et al. (2000), but exhibits only very low catalytic activity in comparison to the native enzyme. In fact, this loss of activity is not surprising. We assume the α-amino group of Ser250 to be mostly protonated (pK_a > 9). Therefore, the amino group is unlikely to act as a base abstracting a proton from Ser250-OH and to provide the major driving force for the activation of its own nucleophile.

The main consequence arising from our study is that the proposed "Ser-only" catalytic mechanism of enzymes of the DmpA family has to be reconsidered. Our results strongly suggest that BapA and DmpA feature catalytic triads (Ser-Ser-Glu and Ser-Ser-Asp, respectively) rather than single catalytic serine residues. This clearly extends the currently proposed catalytic mechanism of DmpA. The importance of these catalytic residues for BapA, DmpA and other DmpA-like proteins is further supported by their high conservation on the structural (Figure 5C) and on the sequence level (Figure 6). Interestingly, despite the close structural similarity of the αββα-sandwich fold, the Ntn hydrolase superfamily comprises enzymes with different catalytic mechanisms. The prototypic Ntn hydrolase penicillin G acylase is reported to have a single catalytic serine residue (Duggleby et al., 1995), the γ-glutamyltranspeptidase from *H. pylori* reveals a threonine-threonine catalytic dyad (Boanca et al., 2007) and the 20S proteasome from *Thermoplasma acidophilum* employs a catalytic tetrad with a threonine residue as primary nucleophile (Löwe et al., 1995).

The presented substrate cleavage mechanism, which is based on mutational and structural data, partially resembles the previously published mechanism by Tikkanen et al. (1996). However, the proposed mechanism for BapA involves a triad of catalytic residues (namely, Glu 290, which activates Ser 250 via Ser 188 for substrate cleavage), whereas the mechanism of Tikkanen et al. (1996) uses a dyad. The presented mechanism for autoproteolytic activation of proBapA differs from recently published mechanisms, such as, for example, the pantetheine hydrolase ThnT. This enzyme is *cis*-autoproteolysed during self-activation (Buller et al., 2012). For self-activation of proBapA, we propose a similar mechanism than for substrate cleavage involving the Ser-Ser-Glu triad. Like already discussed, enzymes having the same Ntn-hydrolase fold do not necessarily act in the same way during substrate cleavage and self-activation (Duggleby et al., 1995; Löwe et al., 1995; Tikkanen et al., 1996; Boanca et al., 2007).

Structure-Based Protein Engineering of β-Aminopeptidases

The superposition of the available crystal structures of β-aminopeptidases (Figure 5C) and a comparison of the biochemically characterized enzymes with related amino acid sequences (Figure 6) showed that despite the highly conserved positions of the catalytically important amino acid residues, the size and chemical environment of the substrate-binding pocket largely differs among these proteins. We expect a nonconserved sequence stretch, assuming different conformations within the substrate-binding pocket, to mainly determine the substrate specificity of proteins of the DmpA-like family. The wide substrate-binding pocket of BapA allows the enzyme to catalyze reactions of peptides with bulky N-terminal β-amino acid residues, while Trp137 in a loop occludes this pocket and

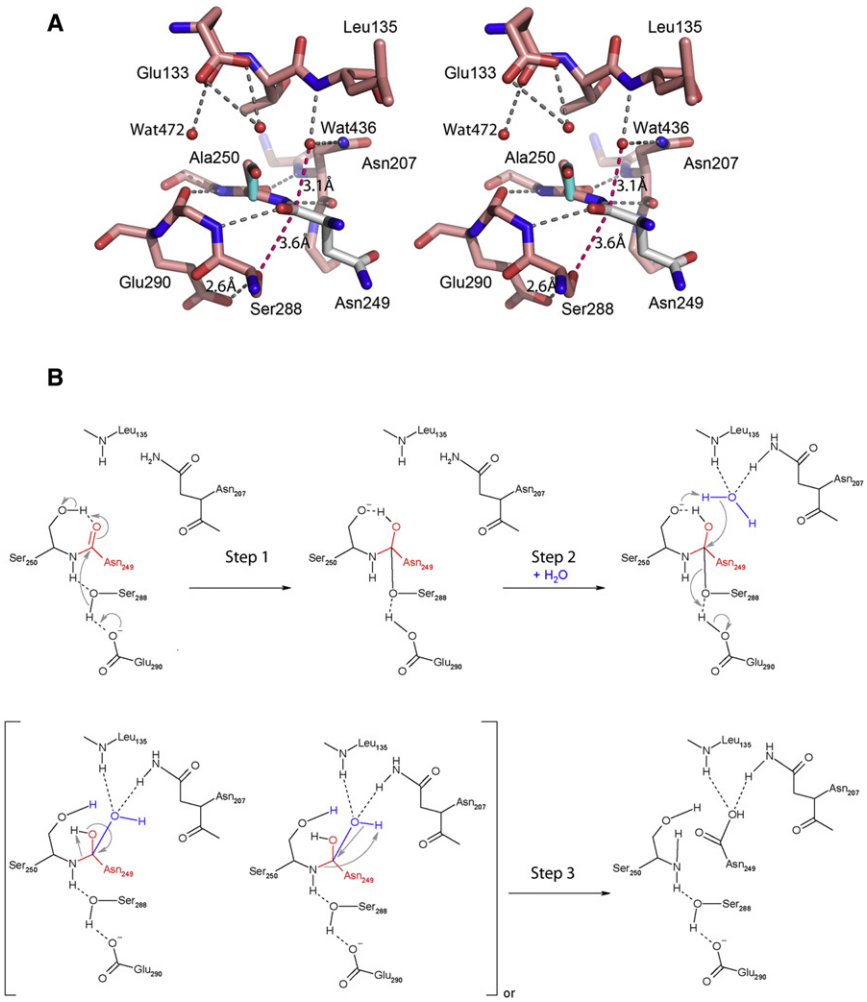

Figure 4. Active-Site Configuration of pro-BapA and Proposed BapA Self-Processing Mechanism

(A) Residues are shown as sticks and water molecules are shown as red spheres. The C-terminal residues of the α chain before autoproteolytic cleavage are shown in gray. Residues important for autoprocessing are labeled. Distances relevant for the mechanism are indicated on the picture.

(B) Step 1: Ser288-Oγ is the nucleophile that is in an ideal position to attack the carbonyl carbon of the Asp249-Ser250 peptide bond to be cleaved. The tetrahedral intermediate formed is stabilized by a hydrogen bond to the Ser250 -Oγ. Step 2: The water oxygen ideally positioned through H-bonds with Asn207-Nδ and the amide nitrogen of Leu135 is the nucleophile that attacks the tetrahedral intermediate resulting in two possible mechanism of cleavage. Step 3: Release of the C terminus of the α-polypeptide; Ser288-Oγ binds the proton back from Glu290.

restricts DmpA to hydrolyze substrates with sterically undemanding N-terminal amino acids. However, by exchanging Trp137 for alanine, DmpA could be rationally engineered to an altered enzyme with catalytic properties that are more similar to BapA than to DmpA (Table 3). Another interesting candidate to study the influence of modifications within the substrate-binding pocket on catalysis is the biochemically noncharacterized protein PH0078 from *P. horikoshii* (PDB ID 2DRH). The active-site loop of PH0078 assumes a similar conformation within the substrate-binding pocket like the corresponding loop of DmpA but exposes a sterically less demanding serine residue instead of a tryptophane toward the active-site residues (Figure 5C). Therefore, we expect PH0078 to exhibit a substrate profile, which is similar to the one of the DmpA mutant W137A. Further specific amino acid exchanges in this particularly variable region might lead to the creation of β-aminopeptidases with interesting novel specificities. The structure-based rational design of modified β-aminopeptidases represents a promising approach to improve the properties of the available enzymes with respect to biocatalytic applications, such as the enzyme-catalyzed synthesis of β-peptides or the production of enantiopure β-amino acids.

EXPERIMENTAL PROCEDURES

Generation of the BapA Duet Expression Constructs and Mutants

The gene sequences coding for the individual α- and β-polypeptide chains of BapA were amplified by PCR from the plasmid p3BapA containing *bapA* from *S. xenopeptidilytica* 3-2W4 without its periplasmic signal sequence (Geueke et al., 2006) and separately cloned into a pETDuet-1 vector (Novagen, Madison, WI) using the following primers:

bapA α chain: fwd 5′-GGAATTCCATGGGGCCGCGCGCTCGCGATCT-3′,
bapA α chain: rev 5′-GGAATTGGATCCTAATTCTTGTCCTGCGGCTTGCCT-3′,
bapA β chain: fwd 5′-GGAATTCCCATATGTCGCTGCTGATCGTGATCGCT-3′,
bapA β chain: rev 5′-GGAATTCTCGAGTCACCGGCGCGGAAACCGCGCCT-3′.

The designated point mutants were generated by site-directed mutagenesis using the QuikChange multi-site-directed mutagenesis kit (Stratagene, La Jolla, CA) with the following primers:

BapA S250A: 5′-CCGCAGGACAAGAATGCGCTGCTGATCGTG-3′
BapA S250C: 5′-CCGCAGGACAAGAATTGCCTGCTGATCGTG-3′
BapA E133A: 5′-CCGGTGGTCGCCGCAACGCTCGACAAC-3′
BapA N249A: 5′-CAAGCCGCAGGACAAGGCTTCGCTGCTGATCGTG-3′
BapA S288A: 5′-GCGGGGGCGCTTGCGGGTGAGTTCGCG-3′
BapA E290A: 5′-GCGCTTTCGGGTGCGTTCGCGCTCGCC-3′
BapA Duet S250A: 5′-GGAGATATACATATGGCGCTGCTGATCGTG-3′
BapA Duet S250C: 5′-GAAGGAGATATACATATGTGCCTGCTGATCGTGATC-3′
BapA Duet E133A: 5′-CCGGTGGTCGCCGCAACGCTCGACAAC-3′
BapA Duet S288A: 5′-GCGGGGGCGCTTGCGGGTGAGTTCGCG-3′
BapA Duet E290A: 5′-GCGCTTTCGGGTGCGTTCGCGCTCGCC-3′.

Expression and Purification of BapA for Biochemical Assays and Protein Crystallization

The production and purification of the β-aminopeptidase BapA from *S. xenopeptidilytica* 3-2W4 and DmpA from *O. anthropi* was done following

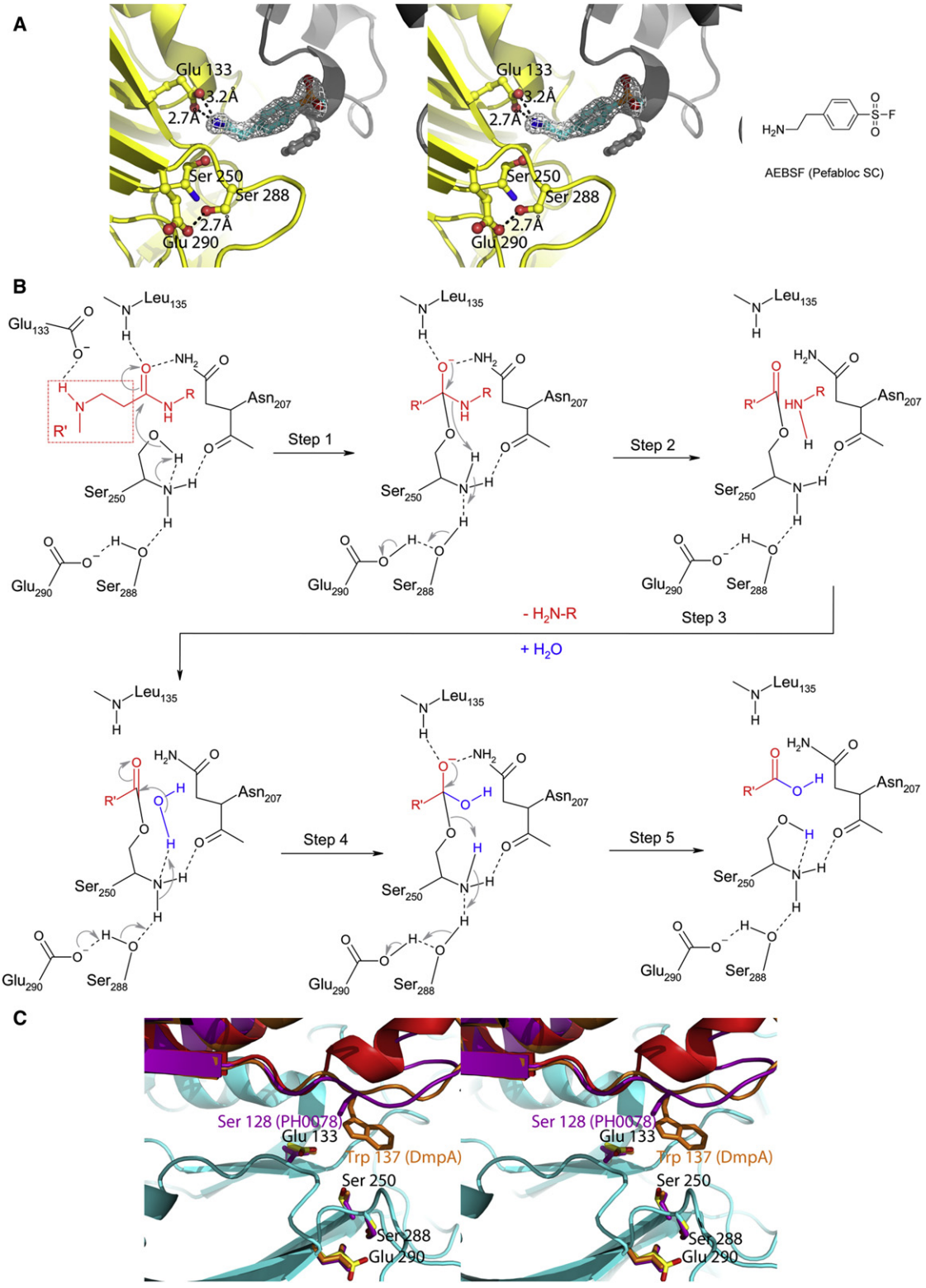

Figure 5. Active Site Configuration and Proposed Substrate Cleavage Mechanism of Native BapA

Stereo representation of the active site configuration of native BapA in presence of the Pefabloc inhibitor (A), proposed catalytic mechanism of substrate cleavage (B) and closeup view into the active-site pocket of native BapA and superposition of BapA with DmpA and PH0078 (C).

(A) The catalytic residues Glu133, Ser250, Ser288, and Glu290 are shown as sticks. Hydrogen bonds are shown as dashed lines. Pefabloc is colored in cyan. The 2fo-fc electron density map around the inhibitor in the active site is contoured at 1.5 σ.

Table 3. Kinetic Analyses of the Conversion of Different β^3-Homoamino-Acid *p*-Nitroanilides by the Purified β-Aminopeptidases BapA, DmpA, and DmpA W137A

	BapA			DmpA			DmpA (W137A)		
Substrate	K_M (mM)	V_{max} (μmol*min^{-1}mg^{-1})	K_{cat}/K_M ($M^{-1}s^{-1}$)	K_M (mM)	V_{max} (μmol*min^{-1}mg^{-1})	K_{cat}/K_M ($M^{-1}s^{-1}$)	K_M (mM)	V_{max} (μmol*min^{-1}mg^{-1})	K_{cat}/K_M ($M^{-1}s^{-1}$)
H-βhGly-*p*NA	6.6 ± 2.3	0.65 ± 0.15	64 ± 37	0.016 ± 0.001	55.8 ± 0.8	2,400,000 ± 200,000	2.9 ± 0.2	20.1 ± 0.5	4600 ± 400
H-β^3hAla-*p*NA	1.1 ± 0.2	16.4 ± 0.9	9,600 ± 1,800	0.063 ± 0.002	109 ± 1	1,200,000 ± 100,000	0.50 ± 0.02	40.0 ± 0.3	53,800 ± 2,100
H-D-β^3hAla-*p*NA			<10[a]	17.0 ± 2.7	1.3 ± 0.2	52 ± 15	0.38 ± 0.13	0.017 ± 0.002	30 ± 13
H-β^3hPhe-*p*NA	3.5 ± 1.3	79.3 ± 14.5	14,500 ± 7,800			<10[a]	0.85 ± 0.09	3.5 ± 0.1	2,800 ± 400
H-D-β^3hPhe-*p*NA			940 ± 3[a]			<10[a]	2.7 ± 0.4	26.7 ± 2.0	6,700 ± 1600

[a]The enzyme activities measured at pH 7.2 and 37°C showed a linear dependency on the substrate concentration between 0.1 and 5 mM. The k_{cat}/K_M values were calculated according to the equation $k_{cat}/K_M = v/(Eo)*[S]$, where v is the rate of the reaction, [S] the concentration of the substrate and (Eo) the stoichiometric concentration of active centers (M_{BapA}: 38,610, M_{DmpA}: 40,440, $M_{DmpA\ W137A}$: 40,330). For the calculation of all kinetic parameters, only the processed enzyme fractions in the protein solutions were taken into account.

established procedures (Geueke et al., 2005, 2006; Fanuel et al., 1999b). All mutants of DmpA, BapA and BapA Duet were purified accordingly. The cell-free extracts and the partially purified proteins were analyzed by SDS-PAGE using precast 10% Novex tricine gels (Invitrogen AG, Basel, Switzerland) according to the manufacturer's instructions. The protein gels were stained with Coomassie Brilliant Blue and the relative intensities of the protein bands were determined with a GS-800 calibrated imaging densitometer and the software Quantity One (Bio-Rad, Reinach, Switzerland). The β-polypeptide chain of partially purified BapA S250 Duet was transferred from the gel to a PVDF membrane by electroblotting and the N terminus was sequenced at the Functional Genomics Center Zürich (Switzerland).

Before crystallization, the purified protein was dialyzed against a 0.5 mM Tris/HCl buffer (pH 8) and concentrated to 15 mg/ml prior to crystallization. Crystals were grown in 2 μl drops with a 1:1 ratio of mother liquor (1.8 M ammonium sulfate and 100 mM Tris/HCl [pH 8]) to purified BapA in 24-well Cryschem sitting-drop plates (Hampton Research, Aliso Viejo, CA) using the vapor-diffusion method at 20°C. Within 1 day, crystals of BapA grew as stacked layers of thin plates. Sequential macroseeding with crystal fragments that were transferred to new wells containing 1.5 M ammonium sulfate, 100 mM Tris/HCl (pH 8), yielded single three-dimensional, mostly plate-shaped crystals of up to 300 × 300 × 30 μm in size. Cryoprotected crystals (mother liquor and 30% glycerol) were flash-frozen in liquid nitrogen.

Structure Determination

Data were collected at the Swiss Light Source beamline PX on a 6M Pilatus detector in a cryostream at 100 K at 1 Å wavelength. The data sets were indexed, integrated and scaled with XDS (Kabsch, 1993). The structure of BapA was solved by molecular replacement with PHASER (McCoy et al., 2007) using one subunit (α and β chain) of the heterooctameric structure of DmpA (PDB ID 1B65). The search probe was additionally tailored at the C terminus of the α chain (residues 224–245). The structure of proBapA was solved by molecular replacement with PHASER using one subunit (α and β chain) of native BapA. The C-terminal tail of the α chain (residues 231–249) was omitted in this search probe. Unambiguous solutions of proBapA and native BapA were obtained, including an extended region of positive difference electron density (Fo-Fc) in the initial map (model phases of BapA and DmpA, respectively) that corresponded to the omitted amino acid linker sequences. Each polypeptide chain comprised 373 amino acids. The final model of native BapA contained residues 1–245/250–371 for chain A, 1–243/250–371 for chain B, 1–245/250–371 for chain C and 1–239/250–371 for chain D. *Ramachandran* statistics: 1,375 (96.6%), 44 (3.1%), and 4 (0.3%) of the residues were in the preferred, generously allowed and disallowed region, respectively. The final model of proBapA contained residues 1–236/248–371 for chain A, 1–236/248–317 for chain B, 1–238/248–371 for chain C and 1–371 for chain D. *Ramachandran* statistics: 1,348 (96.9%), 39 (2.8%), and 4 (0.3%) of the residues were in the preferred, generously allowed and disallowed region, respectively. The refinement of the structures was carried out through multiple cycles of manual adjustments and rebuilding using COOT (Emsley and Cowtan, 2004), and refinement was carried out using PHENIX (Adams et al., 2010). Interface area calculations were performed using the Pisa server v.1.18. Superpositions for figures were done using SSM (Krissinel and Henrick, 2004). Figures were created with the program Pymol (DeLano, 2002).

Activity Assay

The β-aminopeptidase-catalyzed conversion of the β^3-homoamino-acid *p*-nitroanilides H-βhGly-*p*NA, H-β^3hAla-*p*NA, H-D-β^3hAla-*p*NA, H-β^3hPhe-*p*NA, and H-D-β^3hPhe-*p*NA was determined spectrophotometrically by monitoring the release of free *p*-nitroaniline at a wavelength of 405 nm (ε_{405} = 8,800 $M^{-1}cm^{-1}$) for 1 min. For determination of kinetic constants, the assay mixtures contained different molar concentrations of the substrates in a 100 mM

(B) Michaelis complex: Positioning of substrate by electrostatic interactions between the substrate's amino terminus and Glu133. Nucleophilic attack on the carbonyl group of the substrate by Ser250-Oγ, which is activated by Glu290, via Ser288 and the free amino group of Ser250. Step 1: Stabilization of the oxyanion by the backbone amide group of Leu135 and the δNH_2 group of Asn207. Step 2: Substrate cleavage and formation of the acyl enzyme. Step 3: Activation of the catalytic water molecule by Glu133 and initialization of the acyl-enzyme hydrolysis. Step 4: Indirect protonation of the amino group of Ser250 by Glu290 via Ser288 and formation of the second tetrahedral intermediate. Step 5: Hydrolysis of the tetrahedral intermediate, release of the cleaved product, and reconstitution of the active-site residues for another catalytic cycle.

(C) Stereo representation of the active sites of DmpA from *O. anthropi* (PDB ID 1B65) and a noncharacterized protein form *P. horikoshii* (PH0078, PDB ID 2DRH), superimposed onto the structures of BapA from *S. xenopeptidilytica*. The active-site loops containing Ser128 (PH0078) in purple and Trp137 (DmpA) in orange are part of the highly variable sequence stretch of 15–20 amino acids upstream of the conserved Glu133 (BapA numbering). The two subunits forming the active site of BapA are shown in cyan and red, the active-site loops as well as the residues of DmpA and PH0078 are shown as sticks in orange and purple, respectively. The active-site residues Glu133, Ser250, Ser288, and Glu290 of BapA are shown as sticks in yellow. They correspond to Glu135/Glu144, Ser239/Ser250, Ser277/Ser288, and Asp279/Asp290 of PH0078 and DmpA, respectively.

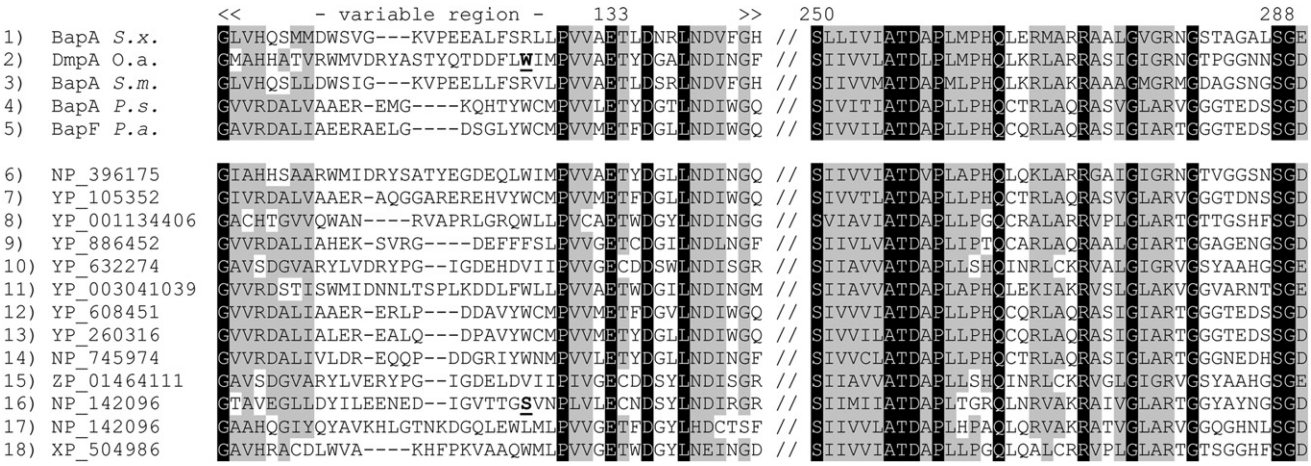

Figure 6. Partial Alignment of β-Aminopeptidase-like Sequences

Sequence alignment of BapA from *S. xenopeptidilytica* with four previously characterized β-aminopeptidases (2–5) and selected, noncharacterized protein sequences that were retrieved from a BLAST search (6–18). Two sections of the alignment are shown (amino acids 104–145 and 250–290). The numbering of the residues refers to BapA from *S. xenopeptidilytica*. Identical amino acids are highlighted in black, similar amino acids are highlighted in gray. Trp137 of DmpA from *O. anthropi*, which was selected as a target for mutagenesis, and Ser128 of the noncharacterized protein PH0078 from *P. horikoshii* (NP_142096) are underlined and printed in bold. The alignment was created with the program ClustalW (Thompson et al., 1994). (1) BapA from *Sphingosinicella xenopeptidilytica* 3-2W4 (AAX93858), (2) DmpA from *Ochrobactrum anthropi* (CAA66259), (3) BapA from *Sphingosinicella microcystinivorans* ABC59253, (4) BapA from *Pseudomonas sp*. MCI3434 (BAE02664), (5) BapF from *Pseudomonas aeruginosa* PAO1 (NP_250177). Noncharacterized protein sequences from (6) *Agrobacterium tumefaciens* C58, (7) *Burkholderia mallei* ATCC 23344, (8) *Mycobacterium gilvum* PYR-GCK, (9) *Mycobacterium smegmatis* MC2 155, (10) *Myxococcus xanthus* DK 1622, (11) *Photorhabdus asymbiotica*, (12) *Pseudomonas entomophila* L48, (13) *Pseudomonas fluorescens* Pf-5, (14) *Pseudomonas putida* KT2440, (15) *Stigmatella aurantiaca* DW4/3-1, (16) *Pyrococcus horikoshii* OT3, (17) *Aspergillus oryzae* RIB40, (18) *Yarrowia lipolytica*.

potassium phosphate buffer (pH 7.2) at 37°C; 10% DMSO was added as cosolvent. The standard assay contained 5 mM H-β^{3}hAla-*p*NA as substrate. The reactions were initiated by the addition of one of the purified enzymes BapA, DmpA, or DmpA W137A, or by the addition of cell-free extract containing recombinantly expressed enzyme. The initial rates of the enzyme-catalyzed release of *p*-nitroanilide were calculated and fitted to the Michaelis-Menten model by nonlinear regression analysis with the VisualEnzymics software (Softzymics, Princeton, NJ) for the program IGOR Pro (WaveMetrics, Oswego, OR).

ACCESSION NUMBERS

The structure data are deposited with the Protein Data Bank with the PDB accession codes 3N5I, 3N2W, and 3N33.

ACKNOWLEDGMENTS

We thank the staff of beamline PX of the Swiss Synchrotron Light Source (PSI) in Villigen, Switzerland for excellent technical assistance. This project was funded by the Swiss National Science Foundation (grants to M.G.G.) and the Swiss NCCR Structural Biology program. T.H. was supported by the Deutsche Bundesstiftung Umwelt (DBU Project No. 13176-32), and B.G. was supported by the Swiss National Science Foundation (SNF Project No. 3152A0-100770). The β-peptidic substrates were a kind gift from D.S. H.-P.E.K. and B.G. conceived the work. T.M. carried out crystallographic data collection, structure determination, and refinement. T.H. and B.G. carried out protein expression, purification, and crystallization experiments. T.H. carried out mutations and kinetic analysis. D.S. and P.R.E.M. contributed to the enzyme mechanism. M.G.G., T.M., and T.H. wrote the paper and prepared the figures with the help of C.B. D.S., M.G.G., B.G., P.R.E.M., and H.-P.E.K. contributed to discussion, data interpretation, and manuscript preparation. M.G.G., B.G., and H.-P.E.K. supervised the work.

Received: May 27, 2011
Revised: June 14, 2012
Accepted: July 15, 2012
Published online: September 13, 2012

REFERENCES

Adams, P.D., Afonine, P.V., Bunkóczi, G., Chen, V.B., Davis, I.W., Echols, N., Headd, J.J., Hung, L.-W., Kapral, G.J., Grosse-Kunstleve, R.W., et al. (2010). PHENIX: a comprehensive Python-based system for macromolecular structure solution. Acta Crystallogr. D Biol. Crystallogr. *66*, 213–221.

Aguilar, M.-I., Purcell, A.W., Devi, R., Lew, R., Rossjohn, J., Smith, A.I., and Perlmutter, P. (2007). β-amino acid-containing hybrid peptides—new opportunities in peptidomimetics. Org. Biomol. Chem. *5*, 2884–2890.

Barends, T.R.M., Yoshida, H., and Dijkstra, B.W. (2004). Three-dimensional structures of enzymes useful for β-lactam antibiotic production. Curr. Opin. Biotechnol. *15*, 356–363.

Baumeister, W., and Lupas, A. (1997). The proteasome. Curr. Opin. Struct. Biol. *7*, 273–278.

Boanca, G., Sand, A., and Barycki, J.J. (2006). Uncoupling the enzymatic and autoprocessing activities of *Helicobacter pylori* γ-glutamyltranspeptidase. J. Biol. Chem. *281*, 19029–19037.

Boanca, G., Sand, A., Okada, T., Suzuki, H., Kumagai, H., Fukuyama, K., and Barycki, J.J. (2007). Autoprocessing of *Helicobacter pylori* γ-glutamyltranspeptidase leads to the formation of a threonine-threonine catalytic dyad. J. Biol. Chem. *282*, 534–541.

Bompard-Gilles, C., Villeret, V., Davies, G.J., Fanuel, L., Joris, B., Frère, J.-M., and Van Beeumen, J. (2000). A new variant of the Ntn hydrolase fold revealed by the crystal structure of L-aminopeptidase D-ala-esterase/amidase from *Ochrobactrum anthropi*. Structure *8*, 153–162.

Brannigan, J.A., Dodson, G., Duggleby, H.J., Moody, P.C.E., Smith, J.L., Tomchick, D.R., and Murzin, A.G. (1995). A protein catalytic framework with an *N*-terminal nucleophile is capable of self-activation. Nature *378*, 416–419.

Bruggink, A., Roos, E.C., and Vroom de, E. (1998). Penicillin acylase in the industrial production of β-lactam antibiotics. Org. Process Res. Dev. *2*, 128–133.

Buller, A.R., Freeman, M.F., Wright, N.T., Schildbach, J.F., and Townsend, C.A. (2012). Insights into cis-autoproteolysis reveal a reactive state formed

through conformational rearrangement. Proc. Natl. Acad. Sci. USA *109*, 2308–2313.

DeLano, W.L. (2002). The Pymol Molecular Graphics System (San Carlos, CA, USA: DeLano Scientific).

Duggleby, H.J., Tolley, S.P., Hill, C.P., Dodson, E.J., Dodson, G., and Moody, P.C.E. (1995). Penicillin acylase has a single-amino-acid catalytic centre. Nature *373*, 264–268.

Elkins, J.M., Kershaw, N.J., and Schofield, C.J. (2005). X-ray crystal structure of ornithine acetyltransferase from the clavulanic acid biosynthesis gene cluster. Biochem. J. *385*, 565–573.

Emsley, P., and Cowtan, K. (2004). Coot: model-building tools for molecular graphics. Acta Crystallogr. D Biol. Crystallogr. *60*, 2126–2132.

Fanuel, L., Goffin, C., Cheggour, A., Devreese, B., Van Driessche, G., Joris, B., Van Beeumen, J., and Frère, J.M. (1999a). The DmpA aminopeptidase from *Ochrobactrum anthropi* LMG7991 is the prototype of a new terminal nucleophile hydrolase family. Biochem. J. *341*, 147–155.

Fanuel, L., Thamm, I., Kostanjevecki, V., Samyn, B., Joris, B., Goffin, C., Brannigan, J., Van Beeumen, J., and Frère, J.M. (1999b). Two new aminopeptidases from *Ochrobactrum anthropi* active on D-alanyl-p-nitroanilide. Cell. Mol. Life Sci. *55*, 812–818.

Frackenpohl, J., Arvidsson, P.I., Schreiber, J.V., and Seebach, D. (2001). The outstanding biological stability of β- and γ-peptides toward proteolytic enzymes: an *in vitro* investigation with fifteen peptidases. ChemBioChem *2*, 445–455.

Fuchs, V., Jaeger, K.-E., Wilhelm, S., and Rosenau, F. (2011). The BapF protein from *Pseudomonas aeruginosa* is a β-peptidyl aminopeptidase. World J. Microbiol. Biotechnol. *27*, 713–718.

Geueke, B., and Kohler, H.-P.E. (2007). Bacterial β-peptidyl aminopeptidases: on the hydrolytic degradation of β-peptides. Appl. Microbiol. Biotechnol. *74*, 1197–1204.

Geueke, B., Namoto, K., Seebach, D., and Kohler, H.-P.E. (2005). A novel β-peptidyl aminopeptidase (BapA) from strain 3-2W4 cleaves peptide bonds of synthetic β-tri- and β-dipeptides. J. Bacteriol. *187*, 5910–5917.

Geueke, B., Heck, T., Limbach, M., Nesatyy, V., Seebach, D., and Kohler, H.-P.E. (2006). Bacterial β-peptidyl aminopeptidases with unique substrate specificities for β-oligopeptides and mixed β,α-oligopeptides. FEBS J. *273*, 5261–5272.

Heck, T., Limbach, M., Geueke, B., Zacharias, M., Gardiner, J., Kohler, H.-P.E., and Seebach, D. (2006). Enzymatic degradation of β- and mixed α,β-oligopeptides. Chem. Biodivers. *3*, 1325–1348.

Heck, T., Kohler, H.-P.E., Limbach, M., Flögel, O., Seebach, D., and Geueke, B. (2007). Enzyme-catalyzed formation of β-peptides: β-peptidyl aminopeptidases BapA and DmpA acting as β-peptide-synthesizing enzymes. Chem. Biodivers. *4*, 2016–2030.

Heck, T., Seebach, D., Osswald, S., Wielter, M.K.J., Kohler, H.-P.E., and Geueke, B. (2009). Kinetic resolution of aliphatic β-amino acid amides by β-aminopeptidases. ChemBioChem *10*, 1558–1561.

Heck, T., Reimer, A., Seebach, D., Gardiner, J., Deniau, G., Lukaszuk, A., Kohler, H.-P.E., and Geueke, B. (2010). β-aminopeptidase-catalyzed biotransformations of β^2-dipeptides: kinetic resolution and enzymatic coupling. ChemBioChem *11*, 1129–1136.

Heck, T., Merz, T., Reimer, A., Seebach, D., Rentsch, D., Briand, C., Grütter, M.G., Kohler, H.-P.E., and Geueke, B. (2012). Crystal structures of BapA complexes with β-lactam-derived inhibitors illustrate substrate specificity and enantioselectivity of β-aminopeptidases. ChemBioChem. Published online September 22, 2012. http://dx.doi.org/10.1002/cbic.201200393.

Johansson, D.G., Wallin, G., Sandberg, A., Macao, B., Aqvist, J., and Härd, T. (2009). Protein autoproteolysis: conformational strain linked to the rate of peptide cleavage by the pH dependence of the N —> O acyl shift reaction. J. Am. Chem. Soc. *131*, 9475–9477.

Kabsch, W. (1993). Automatic processing of rotation diffraction data from crystals of initially unknown symmetry and cell constants. J. Appl. Cryst. *26*, 795–800.

Kim, J.K., Yang, I.S., Rhee, S., Dauter, Z., Lee, Y.S., Park, S.S., and Kim, K.H. (2003). Crystal structures of glutaryl 7-aminocephalosporanic acid acylase: insight into autoproteolytic activation. Biochemistry *42*, 4084–4093.

Kim, J.K., Yang, I.S., Shin, H.J., Cho, K.J., Ryu, E.K., Kim, S.H., Park, S.S., and Kim, K.H. (2006). Insight into autoproteolytic activation from the structure of cephalosporin acylase: a protein with two proteolytic chemistries. Proc. Natl. Acad. Sci. USA *103*, 1732–1737.

Komeda, H., and Asano, Y. (2005). A DmpA-homologous protein from *Pseudomonas sp.* is a dipeptidase specific for β-alanyl dipeptides. FEBS J. *272*, 3075–3084.

Krissinel, E., and Henrick, K. (2004). Secondary-structure matching (SSM), a new tool for fast protein structure alignment in three dimensions. Acta Crystallogr. D Biol. Crystallogr. *60*, 2256–2268.

Löwe, J., Stock, D., Jap, B., Zwickl, P., Baumeister, W., and Huber, R. (1995). Crystal structure of the 20S proteasome from the archaeon *T. acidophilum* at 3.4 A resolution. Science *268*, 533–539.

McCoy, A.J., Grosse-Kunstleve, R.W., Adams, P.D., Winn, M.D., Storoni, L.C., and Read, R.J. (2007). Phaser crystallographic software. J. Appl. Cryst. *40*, 658–674.

McVey, C.E., Walsh, M.A., Dodson, G.G., Wilson, K.S., and Brannigan, J.A. (2001). Crystal structures of penicillin acylase enzyme-substrate complexes: structural insights into the catalytic mechanism. J. Mol. Biol. *313*, 139–150.

Michalska, K., Hernandez-Santoyo, A., and Jaskolski, M. (2008). The mechanism of autocatalytic activation of plant-type L-asparaginases. J. Biol. Chem. *283*, 13388–13397.

Oinonen, C., and Rouvinen, J. (2000). Structural comparison of Ntn-hydrolases. Protein Sci. *9*, 2329–2337.

Saarela, J., Oinonen, C., Jalanko, A., Rouvinen, J., and Peltonen, L. (2004). Autoproteolytic activation of human aspartylglucosaminidase. Biochem. J. *378*, 363–371.

Seebach, D., and Gardiner, J. (2008). β-peptidic peptidomimetics. Acc. Chem. Res. *41*, 1366–1375.

Suresh, C.G., Pundle, A.V., SivaRaman, H., Rao, K.N., Brannigan, J.A., McVey, C.E., Verma, C.S., Dauter, Z., Dodson, E.J., and Dodson, G.G. (1999). Penicillin V acylase crystal structure reveals new Ntn-hydrolase family members. Nat. Struct. Biol. *6*, 414–416.

Thompson, J.D., Higgins, D.G., and Gibson, T.J. (1994). CLUSTAL W: improving the sensitivity of progressive multiple sequence alignment through sequence weighting, position-specific gap penalties and weight matrix choice. Nucleic Acids Res. *22*, 4673–4680.

Tikkanen, R., Riikonen, A., Oinonen, C., Rouvinen, R., and Peltonen, L. (1996). Functional analyses of active site residues of human lysosomal aspartylglucosaminidase: implications for catalytic mechanism and autocatalytic activation. EMBO J. *15*, 2954–2960.

Wiegand, H., Wirz, B., Schweitzer, A., Camenisch, G.P., Rodriguez Perez, M.I., Gross, G., Woessner, R., Voges, R., Arvidsson, P.I., Frackenpohl, J., and Seebach, D. (2002). The outstanding metabolic stability of a ^{14}C-labeled β-nonapeptide in rats—*in vitro* and *in vivo* pharmacokinetic studies. Biopharm. Drug Dispos. *23*, 251–262.

Xu, Q.A., Buckley, D., Guan, C.D., and Guo, H.C. (1999). Structural insights into the mechanism of intramolecular proteolysis. Cell *98*, 651–661.